ISTITUTO NAZIONALE DI FISICA NUCLEARE

Sezione di Milano

INFN/TC-90/12
30 Maggio 1990

G. Gervino, E. Bagnolatti, M. Boero, F. Fasce, M. Icardi, A. Gabutti, C. Manfredotti, E. Monticone:

STUDY ON SILICON DETECTORS

Servizio Documentazione
dei Laboratori Nazionali di Frascati

INFN - Istituto Nazionale di Fisica Nucleare
Sezione di Torino(*)

INFN/TC-90/12
30 Maggio 1990

STUDY ON SILICON DETECTORS

G. Gervino[1)], E. Bagnolatti[1)], M. Boero[1)], F. Fasce[2)], M. Icardi[2)], A. Gabutti[3)], C. Manfredotti[1)] and E. Monticone[4)]

1) Dipartimento di Fisica Sperimentale and INFN Sez. di Torino, Via P. Giuria 1 - 10125 Torino, Italy.

2) Ansaldo Componenti, Div. Semiconduttori, via Lorenzi 8, Genova - Italy.

3) Argonne National Laboratories, Argonne, IL.- USA.

4) IENGF, Strada delle Cacce 90 - 10126 Torino, Italy.

ABSTRACT

Prototypes of silicon microstrip detectors and silicon large area detectors (3x2 cm^2), realized directly by our group, either by ion implantation or by diffusion are presented. The physical detector characteristics and their performances determined by exposing them to different radioactive sources and the results of extensive tests on passivation, where new technological ways have been investigated, are discussed. The calculation of the different terms contributing to the total dark current is reported.

(*) Errata Corrige: Sezione di Torino has been substituted by Sezione di Milano.

1. INTRODUCTION

Solid state detectors are of widespreading use not only in high energy physics, but practically in any branch of laboratory, industry and medical diagnostic activity. Many kinds of detectors may be constructed, depending on the working principle, such as semiconductors detectors, thermoluminescence detectors, etc., but the present work will be related only to silicon detectors and their use as high precision instruments in nuclear and high energy physics[(1–4)]. They are particularly attractive because they achieve high space resolution, are fast devices, can operate in strong magnetic fields and in vacuum, and can match the requests of experiments with geometric constraints. At first, silicon detectors were used in high energy physics as vertex detectors, but recently they have found interesting applications in calorimetry[(5–6)] and in high resolution nuclear physics experiments[(7–8)]. Consequently, big efforts have been undertaken to improve their performance. The drawback of silicon detectors is their high cost (compared to the covered solid angle), to which we must add the cost and the complexity due to the associated electronics read-out. In this paper we discuss about silicon microstrips and large area (3x2 cm^2) detector realized directly by our group either by ion implantation or by diffusion. The detectors with thermally diffused junctions can suggest a cheaper solution, compared to ion implanted devices, in heavy ion nuclear reaction experiments, where wide solid angles are to be covered and very low noise devices are not required.

2. MICROSTRIP DETECTORS

Microstrip detectors achieve an extraordinary space resolution, up to an extent comparable with emulsion, because of the miniaturization possibilities related to the presently available technologies. Also the time resolution (10 - 30 ns.) is high, due to the smaller thickness and to higher electron and hole velocities, compared with other solid state detectors. The microstrip prototypes described in this paper have been built using high purity n-type 3″ silicon wafers, $[1,1,1]$ oriented, 400 μm thick, with a resistivity in the range

$2 - 5\ k\Omega\ cm$, and with doping of $3\ 10^{12}\ cm^{-3}$. The detector area is $2 \times 3\ cm^2$, covered by 100 strips 100 μm wide. The manufacturing stages of ion implanted and diffused microstrips are summarized in Figs. 1 and 2 respectively.

2.1 Diffused strips

The diffused junction was realized in the predeposition step, where a heavily doped p^+ region (around $10^{19} cm^{-3}$) was obtained by thermally diffusing boron atoms at a temperature of about 1060 C for 15′, then decreasing the temperature very slowly for a period of approximately 11 h. Another diffusion (phosphorus) was made to create a back n^+ contact, in order to decrease the series resistance. We measured the junction depth by the spreading resistance technique. The results indicate values between 0.9 and 1.2 μm for different prototypes, with a good depth uniformity for each junction.

2.2 Ion implanted strips

The doping is carried out on both faces by low energy ions (30 keV P, 15 keV B) in doses around $5\ 10^{14}\ ion\ cm^{-2}$. Thin (0.1 μm) self-aligned (implantation is made through a suitable mask) doped regions are realized. A thermal annealing at 600 C is required to remove the introduced radiation damage. The low temperature treatment does not degrade noticeably the carriers life-time.

2.3 Passivation

A 0.4 μm SiO_2 is grown on the crystal surface by exposure to humid oxygen at high temperature (1020 C) for approximately 1 h. Metal impurities and free oxygen atoms are generally responsible for the leakage current. We tried to lower their concentration using HCl as a reducing agent during the oxydation stage. We tested the average resistivity of SiO_2 layer by using the four point technique.

Resistivity values ranged from $7\ 10^8\ \Omega\ cm$ to $3\ 10^{10}\ \Omega\ cm$ for different samples, including deposition done with the same technique. This fact illustrates how crucial the

passivation step is in the realization of silicon detectors. In order to get a better surface passivation and protection, a new process have been investigated during the construction of the large area prototypes, where the technological problems related with the mask alignement are not present. The technological step and the experimental results are described in some details and discussed in section 6. The resistance between adjacent polarized strips, as measured by fixing two micro-probes on them, turned out to be in the range $8000 - 20000\ \Omega$ for ion implanted detectors. Much lower values ($< 1000\ \Omega$) were obtained for diffused ones, due to the higher number of impurities carried on the device surface during the predeposition step, as current density considerations quoted in section 3 further elaborate.

2.4 Photolitography

The geometrical pattern of the various regions of the detectors (doped regions, metallic contacts, etc.) is determined by opening windows in the passivation layer by maens of a photochemical process. A negative photoresistor material has been chosen for its good definition and adherence to the specimen. All the technological processes were carried out in a yellow light room at a constantly controlled humidity (around 25 %) and temperature (20 C). The 'photoresistor' is polymerized by a UV light crossing a well defined mask. The unpolymerized material was taken away by suitable chemical solution. A selective etching is used to remove the underlying SiO_2 in order to open windows. The polymerized material is stripped away by plasma-etch technique, which uses oxygen ions that 'etch' the photoresistor without damaging the specimen.

2.5 Metallization

An aluminium layer of 1.2 μm has been deposed to the detector surface and electrodes have been created by photolitography. The crystal surface has a sufficiently high dopant concentration to get a reasonably good ohmic contact.

The specific resistance R_C, at zero bias, is a figure of merit for ohmic contacts[9]. In this case

$$R = exp[\frac{2\sqrt{\varepsilon_S m}}{\hbar}(\frac{\Phi_S}{\sqrt{N_D}})]$$

where:

m = effective mass of majority carriers

Φ_S = Schottky barrier height ($0.5 - 0.8\ eV$)

N_D = dopant concentration at the interface, which was measured by the spreading resistance technique.

In our case, the experimental value of R_C was approximately $1\ \Omega\ cm^{-2}$.

3. STRIP CHARACTERIZATION

For the diffused detectors we reached a dark current of $100\ nA$ at the depletion voltage of $70\ V$ for a typical strip (see Fig. 3), while, in the case of ion implantation, we got a dark current of $6.5\ nA$ at a depletion voltage of $100\ V$ (see Fig. 4).

The $C - V$ characteristics, from which we can see the depletion of the detector at different reverse applied bias are presented in Figs. 5 and 6, respectively, for ion implanted and diffused strips.

Special considerations are needed for the interpretation of the dark current values and of the evident difference between diffused and ion implanted detectors. We can say that the measured dark current, J_D, is the sum of the following contributors:

$$J_D \cong J_g + J_d + J_s$$

where $J_g = qn_iW/\tau_e$ is the current density due to the charge generation in the depletion region with τ_e carrier life-time ($10^{-3}\ s$), $W = (2\varepsilon_S V/qN_D)^{1/2}$ the depleted region width, ($V = 100\ V$ is the reverse applied bias), J_s is the surface current density, $J_d = qD_h n_i/N_D L_h$ is the diffusion current density, where D_h is the hole diffusion coefficient, L_h the hole diffusion length and N_D the substrate dopant concentration.

We evaluated $J_g \cong 30\ nA\ cm^{-2}$ and $J_d \cong 2\ nA\ cm^{-2}$. These results suggest that the most important contribution to the measured J_D is given by J_s, stressing the importance of passivation and the likely responsibility of the diffusion technique in producing higher concentration of ionized impurities at the surface of the device. This hypothesis is also suggested by the measurements of the strip-to-strip resistance described in section 2.3.

4. STRIP SPECTROSCOPY

We tested the detectors by exposing them to a triple alpha source of Am^{241}, Cu^{244}, Pu^{239}, in a vacuum chamber and by wiring them to the preamplifier described in ref. 10, placed outside the vacuum chamber. The experimental results obtained by ion implanted strip is noted in Fig. 7: a FWHM around 50 keV was reached, with a contribution of the electronic chain noise, as evaluated by the width of the pulser, around 15 keV. Fig. 8 shows the results obtained with the same strip exposed to Ru^{107} beta source, sharply collimated. In Fig. 9 the alpha spectra, for diffused silicon strips, is reported, where only a FWHM around 180 keV for the three alpha emitters quoted before is reached.

5. LARGE AREA PLANAR DETECTOR

Large area silicon detector prototypes for heavy charged particles have been studied and realized in order to suggest a solution for the request of a fast dE/dx device in Nuclear Physics experiments, that will be held at the I.N.F.N. National Laboratories of Legnaro (Italy). We focused our attention on diffusion detectors, trying to optimize the technological process in order to reduce at the minimum the number of thermal treatments that, as it has been pointed out by ref. 11, have a direct negative effect on the carrier life-time of the high resistivity silicon wafers, and, in the end, to build a device as cheap as possible with good resistence to radiation damage, good performance in timing and sufficient

energy resolution. Usually, constructing a large area junction detector, the diffusion is realized on a "mesa" structure or, (less frequently) using the planar technology, a guard ring surrounds the device active area. Both solutions have the goal of lowering the dark current figure (that is the crucial point), but both have important drawbacks. The "mesa" cut on the wafer surface focuses under the junction, in the detector depleted region, the line flux of the applied bias, but the damage done on the crystalline structure increases, proportionally to the depth of the "mesa" cut, the surface current. In the other way, with the planar technology, the construction of a guard ring, keeps apart the detector active area from the rest of the wafer, but at least an additional thermal treatment is required at 1050 - 1250 C, with a negative effect on the carrier life-time, and the corresponding diffusion coefficents of B and P inside the bulk are not negligible. In the following sections large area planar silicon detectors realized without guard-rings are described and discussed.

6. PASSIVATION TEST

The dark current figures, I_D, depend upon the kind of the realized junction, upon the specimen characteristics and, last but not least, upon the surface conditions of the device. The damages on the surface of the crystalline periodic structure bring as a consequence a different distribution of the allowed states in the gap, with respect to the bulk, and increase the probability that impurities diffuse inside. The most important effect related to these phenomena is a dramatic reduction of the carrier life-time. Local alterations of the surface conductivity have been measured and microscopic regions of charge accumulation, both positive and negative, have been seen on the specimen surface. In the worst case, a local inversion of the polarization can be created. To tackle this effect, we studied the performance of SiPOS passivation layer applied to the silicon detector technology. The word SiPOS stands for Silicon-Poly doped with Oxygen. The difference between SiPOS and SiO_2 can be described with the different re-distribution of the carriers at the bulk-insulator interface and with the different behaviour hold by the electric field inside. With SiO_2 the device is badly protected against the electron accumulation at the surface and

against the impurities that can be deposited on the top of the insulator layer. We can see in Fig. 10 a schematic description of the physical effect: it is possible to have a sort of "modulation" from a zone to another one in the surface conductivity . The surface density of state N_{SS} is related to the levels density in the gap, due to sudden interuptions of the periodic crystalline structure, rugged surface, microcracks, etc. These levels, physical traps for the moving carriers, behaves like a sort of recombination centers with a consequent lowering of the carrier life-time. Localized inside the SiO_2, in 200 A from the interface with the bulk and originated by trapped silicon ions,the presence of positive charges Q_{SS} (cm^{-3}) has been found. These ions carry an accumulation of electrons in the n-type wafer, while in the p-type a thin inverse polarized region may be created. The difference from the silicon dielectric constant (ϵ=11.7) and SiO_2 (ϵ=3.6) brings the intersection of the equipotential lines of the applied bias just near the interface SiO_2-Si, moving towards the surface the region where the risk of "breakdown" is higher. In Fig. 11a the effect is shown for the case of a planar detector. In the "mesa" devices this effect is more evident, because the presence of negative Bevel angle may bring the increase of the electric field at the surface. Because the applied bias, in our case, is not going over 150 V, the "breakdown" is a remote possibility, but the increase of the surface density of the line flux grows the dark current figure and causes the deformation of the I-V characteristics. SiO_2 is also sensible to radiation damage, that brings positive ions, created by the incident radiation, to the interface. With the SiPOS all these problems are, in the theoretical way, reduced. When a device is protected by a SiPOS layer, the carriers at the surface may be attracted by the presence of ionized impurities on the top of the insulator and may diffuse inside the insulator, preventing any electric alteration at the bulk interface (see Fig. 11b). The SiPOS layer can be used either on p or n-type wafers and the oxygen used as a dopant acts as a reducing agent for the ohmic current flowing inside the layer: this is a well known effect because the current has a much higher figure for not doped poly-silicon. The minimum figure for the surface current in SiPOS is reached with an oxygen concentration around 15 - 35 percent, and the surface resistivity of the layer range in 10^8-10^9 Ω cm^{-1}. The SiPOS dielectric constant (ϵ_{SiPOS}=11.4 with 20 percent oxygen) helps the decrement of the line flux density when they cross the insulating layer (see Fig. 11b). At present

nothing is known about SiPOS hardness at the radiation damage. In the first tests SiPOS layers were grown with LPCVD technique, directly on the silicon surface at the place of SiO_2 after a chemical cleanning. The low temperature of the process (650 C) avoid the dopant (oxygen) diffusion into the specimen. Up to now does not exist a chemical "etch" that quickly acts only on the SiPOS surface: when the insulator must be stripped away we were obliged to use the same chemical potions useful to attach the silicon and a good knowledge of the reaction time is necessary not to damage the device surface. (The same precautions are necessary whether using "plasma-etch" technique). The I-V characteristics measured on prototypes passivated with SiPOS showed a dark current one order of magnitude higher than SiO_2 and a very "soft" behaviour typical for a high figure of the surface density current. The reason of the pure results experimentally obtained in constrast with the theoretical expectances, was not completely found: we can think that the technological constraints of SiPOS, expecially related to the stripping step, cause a non negligible damage on the detector surface. We got encouraging results combining the properties of SiO_2 with SiPOS (20 percent oxygen). We grew 1 μm SiPOS (LPCVD technique, 650 C) over 0.3 μm SiO_2 and we noticed a dark current around 15 - 20 percent lower than that measured with SiO_2 alone. We think that the SiPOS layer is protecting the SIO_2 from ion contamination at the top; in such a way the passivation strength of SiO_2 is increased and it shows a better action against the surface current. In Fig. 12 the measured I-V characteristic is presented and we can see how its behaviour has a small increment (almost a constant) up to 45 V. In Fig. 13 the detector C-V behaviour is shown, and Fig. 14 and 15 show the detector response when irradiated with a triple alpha emitters (Pu^{239}, Am^{241} and Cm^{244}) and a Am^{241}-source alone: in the case of the triple alpha source the three peaks are well observed, and from the the Am^{241} peak of Fig. 15, taken in the same electronic conditions used for Fig. 14, a FWHM energy resolution of about 370 keV has been measured.

6. CARRIER LIFE-TIME

If we assume for a while that the most important contribution to the device measured

dark current density J_D is the charge generation current in the depleted region, we get for the carrier life-time a figure much less than that we had for the bulk (10^3 μm guaranteed by the manufacturer). If we define

$$J_{gen} = \frac{1}{2}\frac{n_i q W}{\tau_0}$$

and if we consider an applied bias of, for instance, 40 V (see Fig. 12), we have for J_{gen} 12 10^{-6} A/cm^2 and τ_0 equal to 4 10^{-8} sec. We can explain this result considering the effect of the thermal treatments on the bulk and the dependence of the carrier life-time from the carrier concentration. In the case of very thin n^+-p junctions, with a donor concentration of $N_D > 10^{19}$ cm^{-3} and a constant surface recombination rate, it is possible to evaluate the effects that the combined phenomena of generation - recombination have on the life-time from the relationship:

$$\tau_n = \frac{\tau_0}{\frac{1+N}{N_{A0}}}$$

This allows us to compute for our n^+-p junction $\tau_n \cong 10^{-8}$ sec. The measured values for τ are in the range of 10^{-6} - 10^{-7} sec. The effects of thermal treatments on the bulk are still up to now a matter of investigation, but we observed (according qualitatively with ref. 9) an effective lowering of the carrier life-time depending upon the temperature. It is necessary to distinguish between the effects induced on the crystalline lattice and the effects related to the diffusion of impurities either inside the bulk or towards the surface. Building a diffused junction requires technological steps with temperatures greater than 1000 C, and we measured that the carrier life-time decreases more drastically after the first thermal ossidation than during the boron or phosphorus deposition. The high temperature is carrying on the lattice new and higher density of damages and the crystalline vacancies diffuse. The discrepancy between the two theoretical values computed for τ (4 10^{-8} and 10^{-8}) and the experimental figure (10^{-6}, 10^{-7}) may be explained, according with the calculation done in section 3, saying that the most contributor to the measured dark current is not the generation current. But this does not explain more than 1000 times decrement from the bulk starting figure. We did few tests on intrinsic silicon samples "float-zone", and it was observed τ_n passing from 200 μs to 7 μs after a treatment at 800 C. In conclusion it

is reasonable to think that the thermal treatments bring a strong alteration in the carrier life-time and the way of improving the detector electric characteristics must consider the possibility of minimizing them in number and in temperature.

7. CONCLUSIONS

Ion implanted multistrip detectors are a very powerful high precision instruments for nuclear and high energy physics. The method of improving their performance surely has to face with the technological improvements of the passivation step, in order to further lower the surface current density J_s, that, as we pointed out, gives the largest contribution to the total dark current. Diffused detectors display higher dark currents, likely due to the surface impurities penetrating into the device during the deposition step, and also to the high temperature ($> 1000\ C$) thermal treatments required by their manufacturing process. The performance of diffused detectors, joined with their lower cost, can match the needs of calorimetry, as well as high resolution nuclear experiments, where wide solid angles are to be covered.

ACKNOWLEDGEMENTS

We are indebted to the technical staff of the I.R.C.I. - International Rectifier of Torino. We would like to thank above all Dr. Aldo Torti, I.R.C.I. chief-responsible, Dr. Marcello Turnaturi, I.R.C.I. technical responsible, Mr. Luigi Merlin and Mr. Giovanni Righieri. We also have to thank Dr. F. Zani and Ing. M. Zambelli of ANSALDO Trasporti, Div. Semiconduttori, where part of the passivation tests were performed. The implantation step was carried out at LAMEL laboratory (Bologna - Italy), by Dr. F. Zignani and A. Cembali.

REFERENCES

1. G. Bertolini and A. Coche, Semiconductor detectors, North Holland (1968)
2. S. Deme, Semiconductor detector for nuclear radiation measurements, Hilghar Ltd., London (1971).
3. P. G. Rancoita and A. Seidman, La Rivista del Nuovo Cimento, vol. 5, n. 7 (1987).
4. E. Heijne, L. Hubbeling, B. Hyams, P. Jarron, P. Lazeyras, F. Puiz, J. Vermeulen and A. Wylie, Nucl. Instr. and Meth. A178, 331 (1980).
5. G. Barbellini, P. Buksh, G. Cecchet, J. Y. Hemery, F. Lemeilleur, P. G. Rancoita, G. Vismara and A. Seidman, Nucl. Instr. Meth. A235, 216 (1985).
6 A. Nakamoto, H. Murakami, T. Doke, J. Kikuchi, K. Masuda, K. Kasahara, K. Mitsui, Y. Muraki and T. Yuda, ICR Report 118/84/7, (November 1984).
7 P. Doll, G. Fink, F. Brady, G. Garrett, H. O. Klages and H. Krupp, Nucl. Instr and Meth. A250, 526 (1986).
8. M. Anghinolfi, M. Castoldi and A. Rottura, Il Nuovo Cimento, vol. 98A, n. 5 (1988)
9. S. M. Sze, Physics of semiconductors devices (Wiley, New York, 1981), pag. 304.
10. C. Manfredotti, A. Crosetto, A. Gabutti, G. Gervino, E. Monticone and L. Brunetti, Nucl. Instr. and Meth. A261, 527 (1987)
11. W. Graff and H. Peiper, Journal of Electronic Materials, Vol. 4, N. 2 (1976).

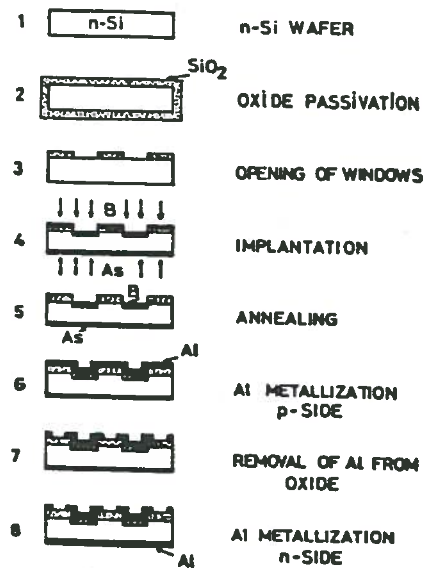

Fig. 1 : Planar technology for implanted strip detectors.

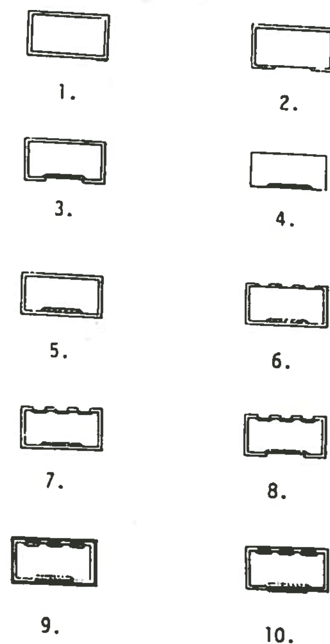

Fig. 2 : Planar technology for diffused strip detectors: 1) Oxide passivation, 2) Window opening, 3) diffusion of P, 4) Oxide removal, 5) Oxide passivation, 6) Strip window opening, 7) Diffusion of B, 8) Etching, 9) Aluminium deposition, 10) Contacts.

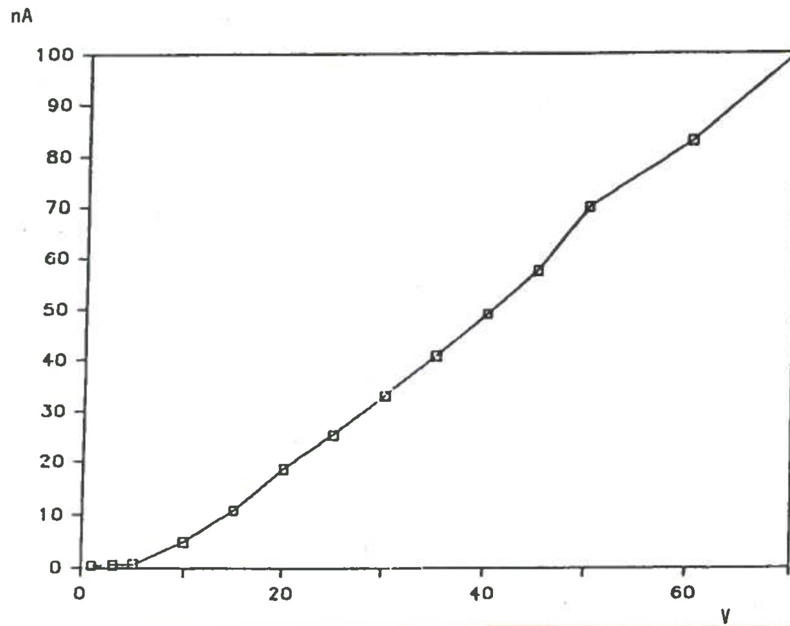

Fig. 3 : $I - V$ characteristic of a typical diffused silicon strip.

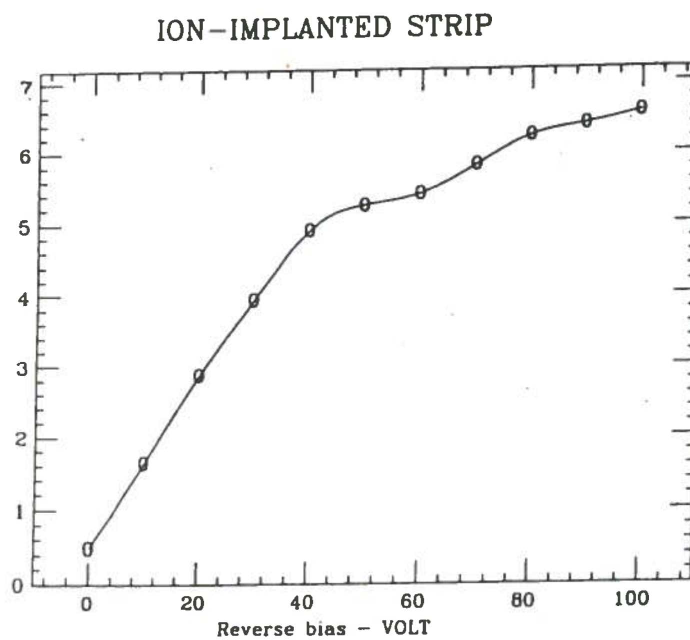

Fig. 4 : $I - V$ characteristic of a typical ion implanted silicon strip.

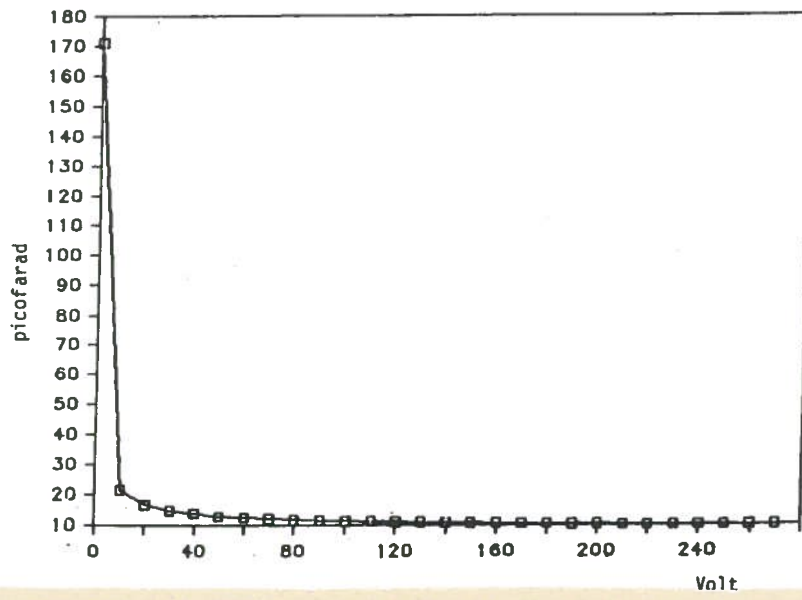

Fig. 5 : $C - V$ characteristic of a typical diffused silicon strip.

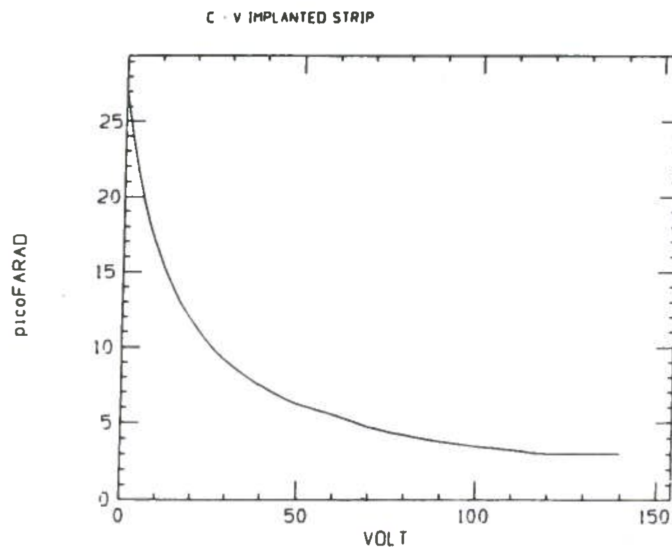

Fig. 6 : $C - V$ characteristic of a typical ion implanted silicon strip.

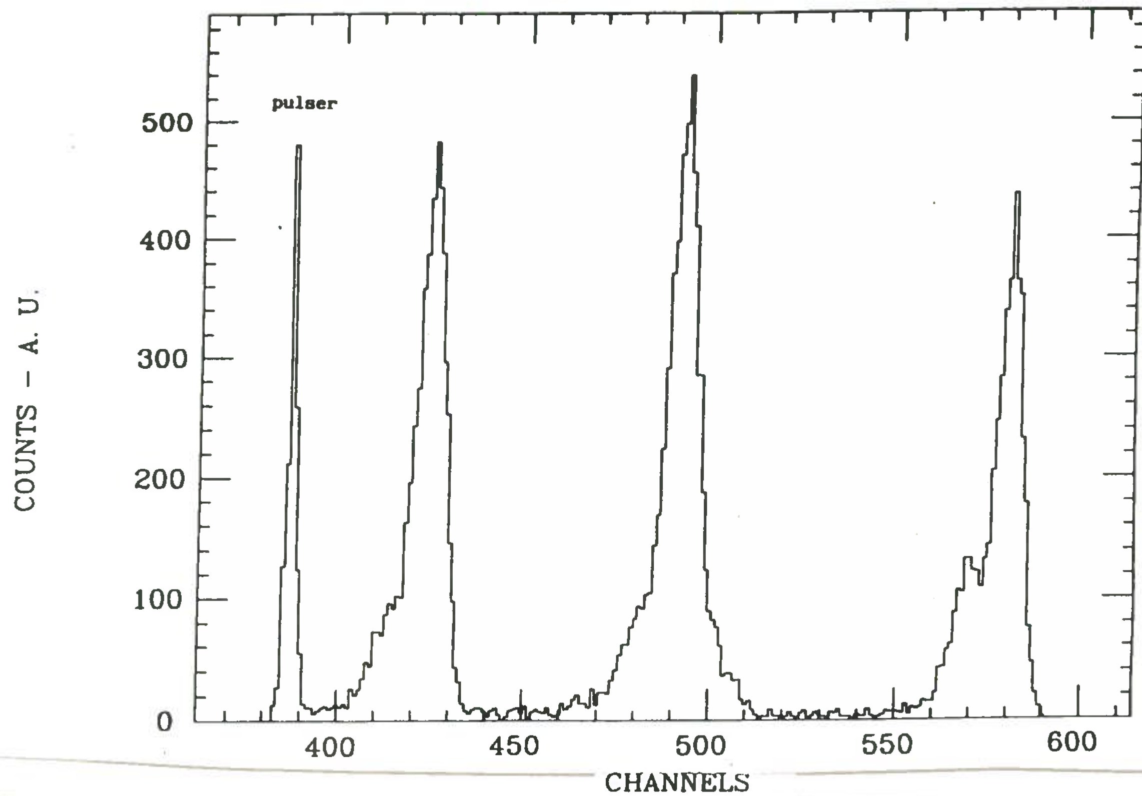

Fig. 7 : Alpha spectra obtained from ion implanted strip detector. The FWHM of the pulser, giving the contribution of the electronic chain noise, is approximately 15 keV.

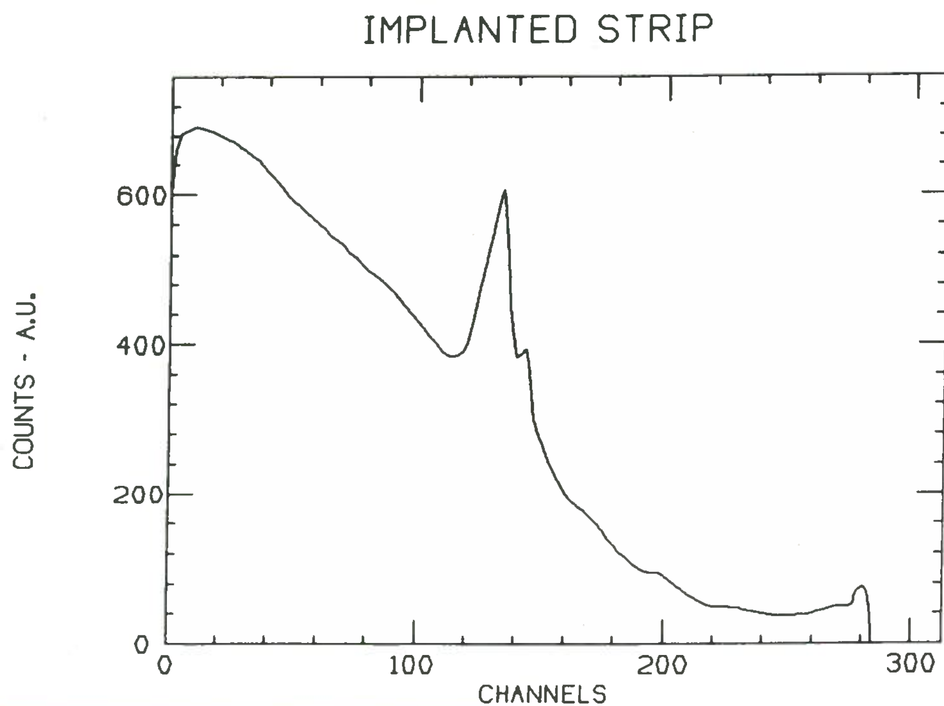

Fig. 8 : A collimated Ru^{107} beta spectrum obtained from the ion implanted strip detector.

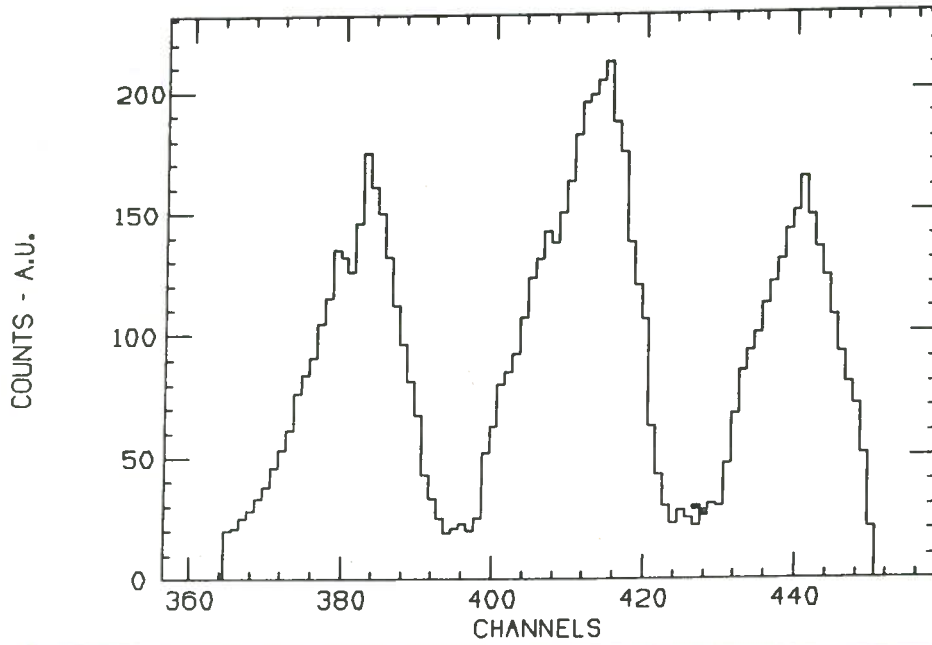

Fig. 9 : Alpha spectra from the diffused strip detector.

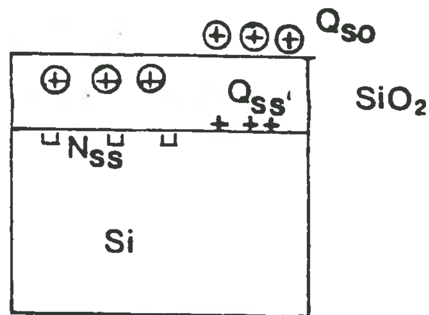

Fig. 10 : Schematic representation of the effect related to electron accumulation at SiO_2-bulk interface and related to ionized impurities deposited on the top of the passivation layer.

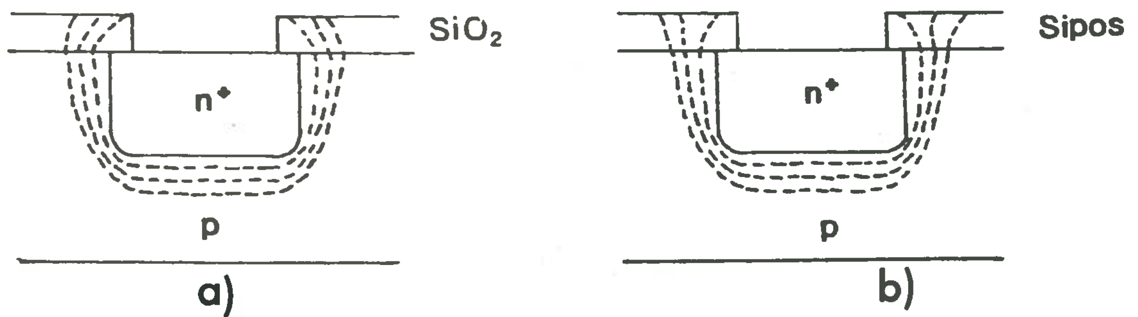

Fig. 11 a): Behaviour of the equipotential line for a n^+-p junction passivated with SiO_2. b): Same behaviour with SiPOS passivation.

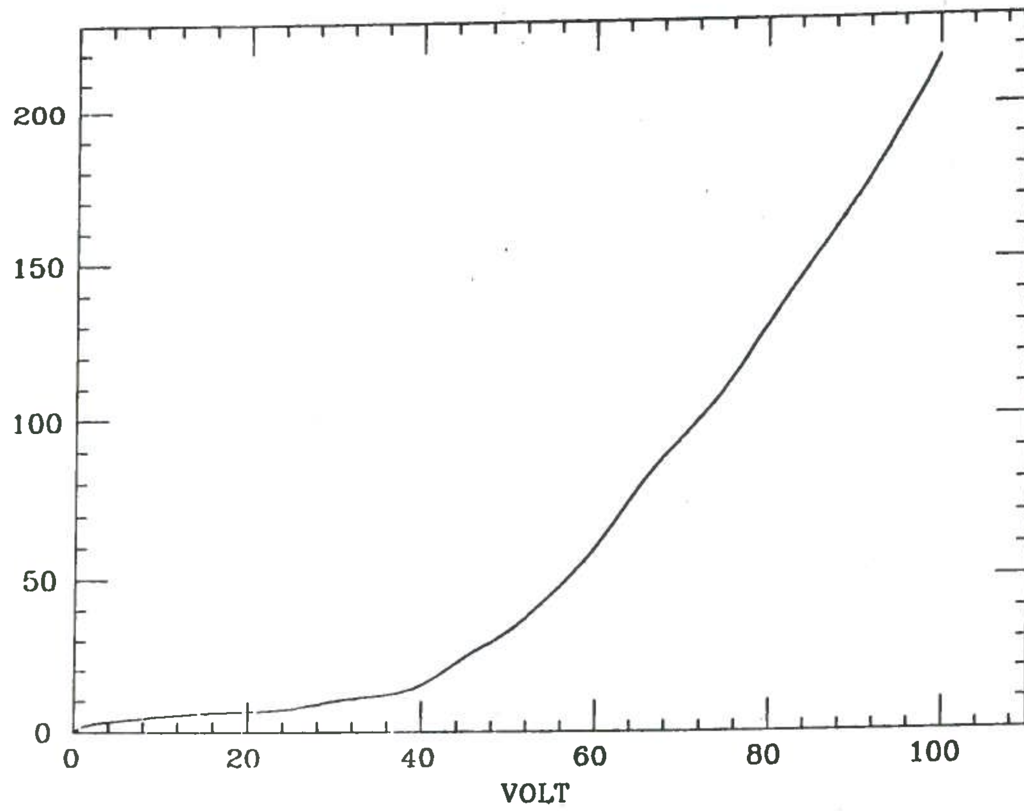

Fig. 12 : I-V characteristics of 3x2 cm^2 planar silicon detector.

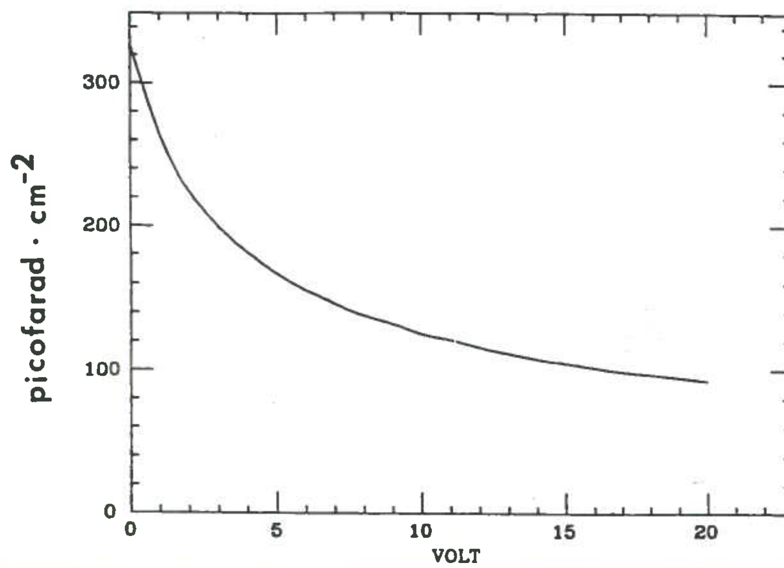

Fig. 13 : C-V characteristic of a large area silicon detector prototype.

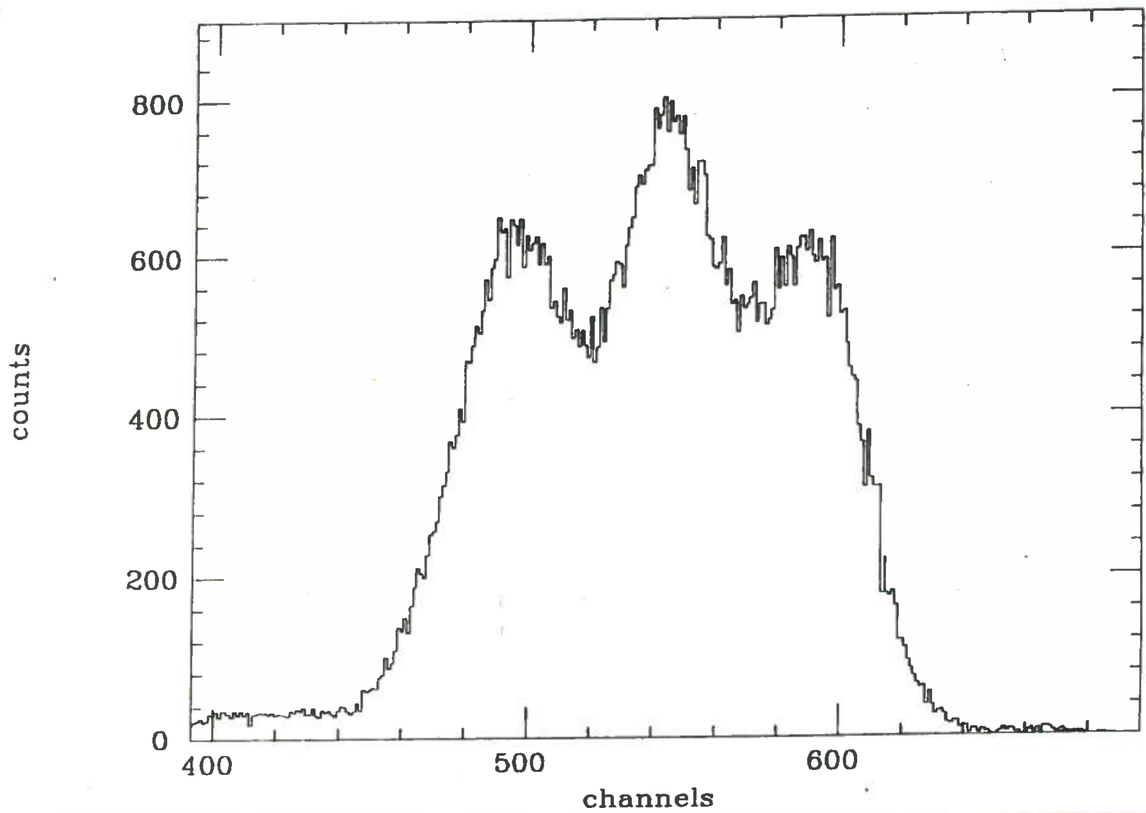

Fig. 14 : Alpha spectra obtained from Pu^{239}, Am^{241} and Cm^{244}emitters.

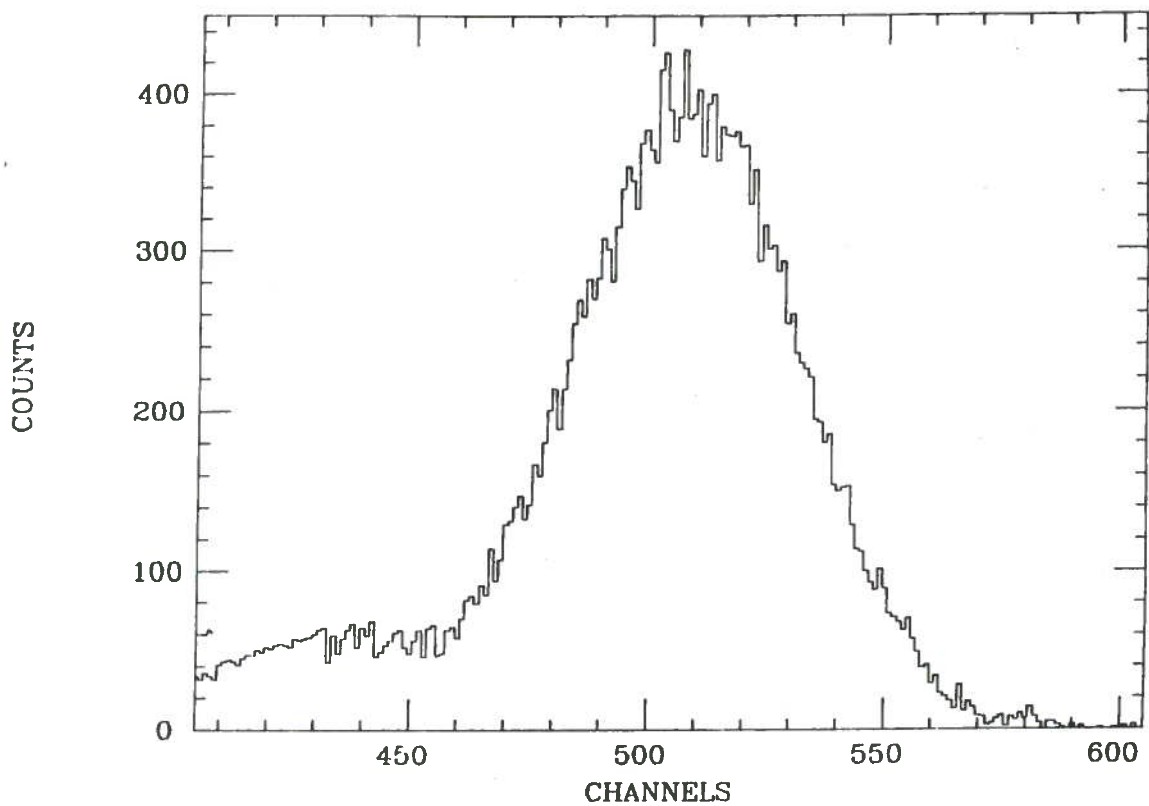

Fig. 15 : Alpha peak from Am^{241} source measured in the same electronic conditions of Fig. 14. The FWHM energy resolution is around 370 keV.